Rate Constants for the Reactions of ATP- and ADP-Actin with the Ends of Actin Filaments

Thomas D. Pollard

Department of Cell Biology and Anatomy, Johns Hopkins Medical School, Baltimore, Maryland 21205

Abstract. I measured the rates of elongation at the barbed and pointed ends of actin filaments by electron microscopy with *Limulus* sperm acrosomal processes as nuclei. With improvements in the mechanics of the assay, it was possible to measure growth rates from 0.05 to 280 s^{-1}. At 22°C in 1 mM $MgCl_2$, 10 mM imidazole (pH 7), 0.2 mM ATP with 1 mM EGTA or 50 μM $CaCl_2$ or with EGTA and 50 mM KCl, the elongation rates at both ends have a linear dependence on the ATP-actin concentration from the critical concentration to 20 μM. Consequently, over a wide range of subunit addition rates, the rate constants for association and dissociation of ATP-actin are constant. This shows that the nucleotide composition at or near the end of the growing filament is either the same over this range of growth rates or has no detectable effect on the rate constants. Under conditions where polymerization is fastest ($MgCl_2$ + KCl + EGTA) the rate constants have these values:

	ATP-actin		ADP-actin	
	Barbed	Pointed	Barbed	Pointed
k_+ ($\mu M^{-1}s^{-1}$)	11.6	1.3	3.8	0.16
k_- (s^{-1})	1.4	0.8	7.2	0.27

Compared with ATP-actin, ADP-actin associates slower at both ends, dissociates faster from the barbed end, but dissociates slower from the pointed end. Taking into account the events at both ends, these constants and a simple Oosawa-type model account for the complex three-phase dependence of the rate of polymerization in bulk samples on the concentration of ATP-actin monomers observed by Carlier, M.-F., D. Pantaloni, and E. D. Korn (1985, *J. Biol. Chem.*, 260:6565-6571). These constants can also be used to predict the reactions at steady state in ATP. There will be slow subunit flux from the barbed end to the pointed end. There will also be minor fluctuations in length at the barbed end due to occasional rapid dissociation of strings of ADP subunits but the pointed end will be relatively stable.

THE mechanism of actin polymerization has been studied in detail (see reviews by Korn, 1982; Frieden, 1985; Pollard and Cooper, 1986), both because it is a model for other macromolecular self-assembly reactions and because knowledge about actin polymerization is a limiting factor in understanding the mechanisms of all of the actin-binding proteins. The goal of this work on actin is a full quantitative model for polymerization that includes the rate constants for each step. Spontaneous polymerization from actin monomers involves several unfavorable nucleation steps that are rate limiting and much more rapid elongation reactions in which actin molecules bind to and dissociate from the two ends of the filaments. Much more is known about elongation than nucleation, because there are direct methods to measure elongation but not nucleation.

There are still open questions about elongation, because we have not had reliable values for all of the rate constants and there is some uncertainty about the number of the reactions. At the very least, we must know nine different rate constants: the association and dissociation rate constants for ATP-actin and ADP-actin from both the fast (barbed) end and the slow (pointed) ends of the actin filaments and the rate constant for ATP hydrolysis by polymerized ATP-actin molecules. Many of the elongation rate constants have been measured (Pollard and Mooseker, 1981; Bonder et al., 1983; Coluccio and Tilney, 1983; Pollard and Weeds, 1984; Doi and Frieden, 1984; Pollard, 1984; Lal et al., 1984*a*, *b*; Carlier et al., 1984; Coue and Korn, 1985; Selve and Wegner, 1986; Carlier et al., 1986*a*, *b*). However, as discussed by Coue and Korn (1985), the published values of the constants for ATP-actin and ADP-actin at the slow (pointed) end of the filament are problematic, because it has been difficult to interpret solution experiments where capping proteins (Doi and Frieden, 1984; Coue and Korn, 1985; Selve and Wegner, 1986) or cytochalasin (Carlier et al., 1986*a*, *b*) were used to inhibit reactions at the barbed end. Complications with these assays have precluded the direct determination of the dissociation rate constant for ATP-actin at the pointed end in bulk samples (Coue and Korn, 1985; Carlier et al., 1986*a*, *b*).

In reality the nine minimal rate constants may not account for all of the important reactions involved in the elongation

process. For example, Pantaloni et al. (1985*a*, *b*) point out that the association and dissociation rate constants may depend not only on the nucleotide content (ATP vs. ADP) of the reacting subunit but also on the nucleotide content of neighboring subunits at the ends of the filament. Furthermore, the rate constant for ATP hydrolysis by polymerized ATP-actin may depend on the nucleotide composition of the neighboring subunits. Pantaloni et al. (1985*a*, *b*) proposed a sophisticated model with several interesting features that can account for the complex dependence of the elongation rate in bulk samples on the concentration of ATP-actin. For the present discussion, there are two important features of their model. First, the rates of association and dissociation of actin from the ends of filaments are highly dependent on the nucleotide composition of the two terminal subunits; ATP-actin binds tighter to an end where only the two adjacent subunits have ATP than to an end with a large "cap" of ATP subunits. Second, the rate of ATP hydrolysis is much higher on actin subunits located at a boundary between the internal ADP-actin core and the ATP-actin "cap" near the end of growing filaments than on either internal subunits surrounded by other ATP-actins or on the two terminal ATP subunits at the end of the filament.

To test whether these complications are important, I used electron microscopy and improved techniques for specimen preparation to evaluate directly over a wide range of monomer concentrations the rate constants for the association and dissociation of ATP- and ADP-actin at both ends of the actin filament. The result is that these elongation rate constants are constant over a wide range of reaction rates. One interpretation is that the nucleotide composition of the actin molecule that binds or dissociates is the major determinant of the reaction rates and that the nucleotide composition of the adjacent subunits at the ends of the filament does not have a detectable effect on the elongation reactions. When one takes the reactions at both the barbed and pointed ends into account, a simple mechanism can account for the complex polymerization curves of Carlier et al. (1985) and Pantaloni et al. (1985*b*). Further, the availability of a complete set of rate constants makes it possible to predict events at steady state. In ATP, KCl, $MgCl_2$, and EGTA there will be a slow flux of subunits from the barbed end to the pointed end, but this flux will be damped by the slow dissociation of ADP-actin from the pointed end.

Materials and Methods

Protein Purification

Actin was purified from rabbit skeletal muscle (Spudich and Watt, 1971) and monomers were separated from oligomers and minor contaminants by gel filtration on Sephadex G-150 (MacLean-Fletcher and Pollard, 1980). ATP-actin was stored in Buffer G (2 mM imidazole [pH 7.5], 0.5 mM dithiothreitol [DTT], 0.2 mM ATP, 0.1 mM $CaCl_2$, 0.5 mM NaN_3) at 4°C and used within 1 wk. Mg-ATP-actin was prepared at a concentration of 20 μM by adding $MgCl_2$ to a concentration of 50–80 μM and EGTA to 125–250 μM and incubating at 4°C for 10–20 min. Mg-ADP-actin was prepared by the Selden et al. (1986) modification of the method of Pollard (1984) as follows. Mg-ATP-actin was incubated with 20 U/ml of yeast hexokinase and 1 mM glucose for 4 h at 4°C. Part of this 20 μM Mg-ADP-actin was reconverted to Mg-ATP-actin by diluting to 5 μM into Mg-EGTA buffer with 1 mM ATP and incubating for 75 min at 4°C. The final concentrations were 0.55 mM ATP, 0.25 mM ADP, and 0.25 mM glucose-6-phosphate.

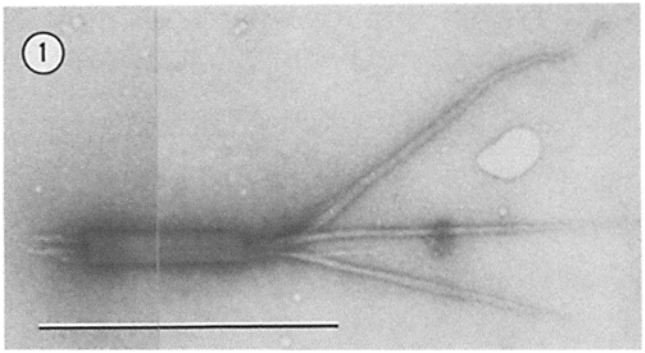

Figure 1. Electron micrograph of actin filaments grown from the ends of *Limulus* acrosomal processes and then bundled just before staining by treatment with 5 mM spermine. Solution conditions as in Fig. 2, 17.5 μM ATP-actin for 4 s. The center of the acrosomal process is cropped to save space. Bar, 1 μm.

Elongation Rates

Electron microscopy was used to measure the rates of elongation at the two ends of the actin filament. The present method is a modification of and a substantial improvement over the methods used previously (Pollard and Mooseker, 1981; Bonder et al., 1983; Pollard and Cooper, 1984). *Limulus* sperm acrosomal processes (APs)[1] were used as morphologically identifiable nuclei. The APs were isolated from fresh sperm by a modification of the method of Tilney (1975). About 100–200 μl of sperm were washed three or four times in 1.5 ml of ice cold, filtered sea water by centrifuging 5 s in an Eppendorf Model 5414 centrifuge. This 11,000 *g* spin pelleted the sperm and left contaminating cells, immature sperm, and debris in the supernatant. The pelleted sperm were resuspended very gently with a Pasteur pipet to avoid lysis of the nuclei. The sperm were then resuspended very gently in 1.5 ml of ice cold 30 mM Tris-Cl (pH 8.0), 3 mM $MgCl_2$, 1% Triton X-100, and centrifuged for 15 s in the Eppendorf centrifuge. This pelleted the nuclei and axonemes, leaving the APs in the supernatant. The APs were washed free of soluble materials and detergent by pelleting twice in the Eppendorf centrifuge for 7 min. The buffer for washing and final resuspension of the APs was 2× polymerization buffer, generally 100 mM KCl, 2 mM $MgCl_2$, 2 mM EGTA, 20 mM imidazole (pH 7.0). The APs for polymerization of actin-ADP were washed in buffer with hexokinase and glucose. The APs in 300–500 μl of buffer were vigorously forced five times through a 25-gauge needle to break them into short pieces. A fresh preparation was made each day.

The polymerization reaction was carried out at room temperature (22°C) in a small droplet on parafilm with the electron microscopy grid floating on the surface. First, 15 μl of APs in 2× buffer were applied to the parafilm. Second, a freshly glow discharged, carbon-formvar-coated EM grid was floated on the surface or held there with fine forceps. Third, the reaction was started by rapidly pipetting 15 μl of actin monomer into the droplet and mixing by pipetting in and out three times as fast as possible (generally <0.5 s). Fourth, 1.5 s before the end of the incubation time the grid was lifted from the droplet and its edge was dragged at an angle of 45° across filter paper to remove excess fluid. A thin film of reaction solution remained on the grid providing that the grid was hydrophilic. Fifth, precisely at the end of the incubation time the grid was inverted onto a 250-μl drop of 1× polymerization buffer with 5 mM spermine (pH 7.0). This rapidly diluted thin film of reactants on the grid and stopped the reaction. The spermine aggregated the filaments that had grown from the ends of the APs into one or several bundles that tapered sharply near their tips (Fig. 1). After 5–10 s in spermine, excess fluid was again removed from the grid with filter paper and the grid was inverted onto a drop of 1% uranyl acetate for 5 s. After removing all but a thin film of stain, the grids were air dried. One person could easily prepare samples incubated 10 or more seconds. Two people were required for shorter time points, especially since the incubation must then be timed with a stop watch. The shortest practical incubation time was ~4 s. If the time points were separated by 30 s or more, the drop size could be increased and up to four grids could be floated on a single drop. Routinely two or three time points were obtained for each concentration of actin.

1. *Abbreviation used in this paper*: APs, acrosomal processes.

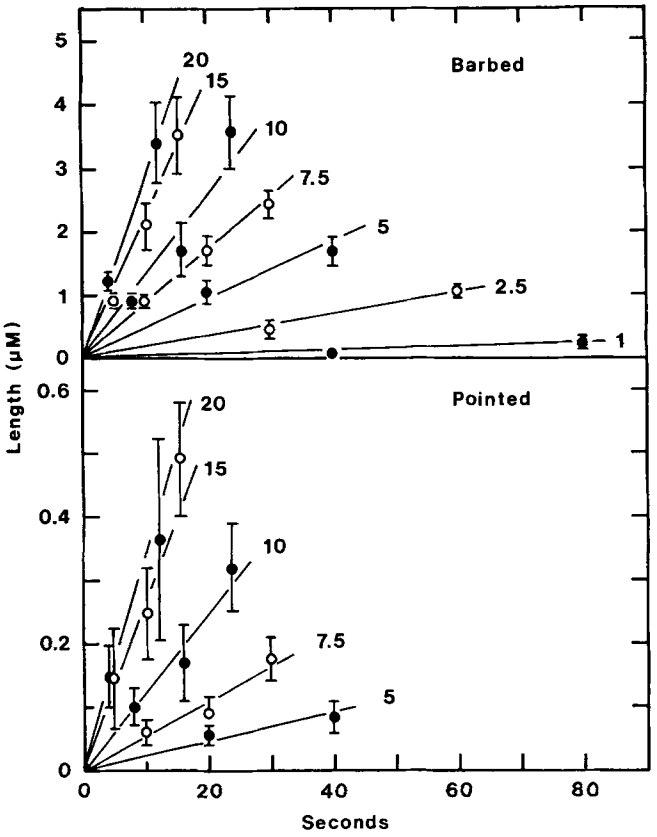

Figure 2. Time course of the growth of actin filaments from the barbed and pointed ends of acrosomal processes. Conditions: 1 mM $MgCl_2$, 50 μM $CaCl_2$, 0.3 mM ATP, 0.25 mM DTT, 10 mM imidazole (pH 7), 22°C. The actin monomer concentration (μM) is given beside each plot. Vertical bars are ±1 standard deviation.

When the reaction rate was slow (<30 s^{-1} at the barbed end), only two time points were necessary because the reaction rates were always linear and highly reproducible.

The length of the bundles at the two ends of the APs were measured by electron microscopy directly on the viewing screen at a magnification of 4,500 or 8,900. This was done visually for lengths between 0.5 and 4.5 μm by comparing the length of the actin bundle with radius or diameter of the field. For lengths up to 2.5 μM, the method was accurate to within 0.1 μm. Between 2.5 and 4.5 μm, the measurement was accurate to within 0.2 μm. Lengths between 0.05 and 0.5 μM were estimated within 0.05 μm by comparison with cross marks in the center of the screen which were 0.25 and 0.47 μm long. It was possible to use this rapid method rather than photography, because the bundles of actin filaments were straight or only gently curved.

For each time point, the length of the bundles on at least 20 separate APs were recorded. The long end is the barbed end and the short end the pointed end (Bonder et al., 1983). Since there are a number of artifacts produced by this method, some APs had to be rejected from inclusion in the data sets. These artifacts included obvious fractures of the bundles (indicated by straight rather than tapered ends or no bundle at all at the barbed end) and annealing of bundles of separately nucleated filaments to the ends or sides of bundles nucleated by the AP (indicated by grossly uneven lengths of the several bundles on one AP or between APs). This latter artifact occurred when high actin concentrations were incubated for long times and was presumably due to spontaneous nucleation. The problem was avoided by limiting the time of incubation, so that there were few or no free actin filaments in the background on the grid (e.g., <10 s for 20 μM actin in KCl-Mg-EGTA).

For each actin concentration, the mean length was plotted vs. time to obtain the rate of growth. The slopes of these plots were the elongation rates. The association and dissociation constants and critical concentration were obtained from least squares linear regression of plots of growth rate vs. actin monomer concentration (Pollard and Mooseker, 1981).

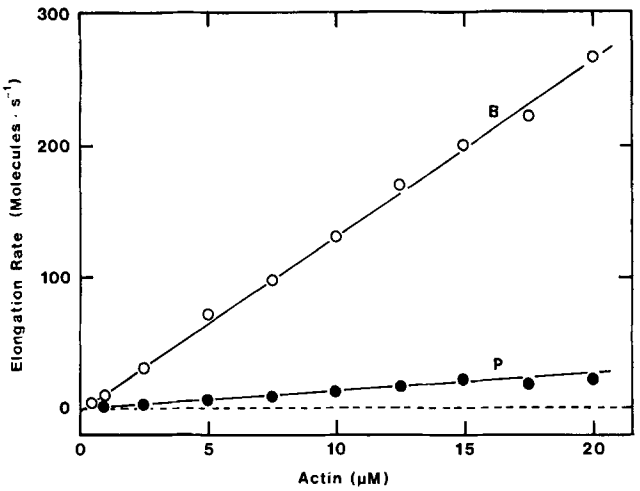

Figure 3. Elongation rates at the barbed (*open circle*) and pointed (*solid circle*) ends of actin filaments as a function of the actin monomer concentration. Conditions: 50 mM KCl, 1 mM $MgCl_2$, 1 mM EGTA, 50 μM $CaCl_2$, 0.2 mM ATP, 0.5 mM DTT, 10 mM imidazole (pH 7), 22°C.

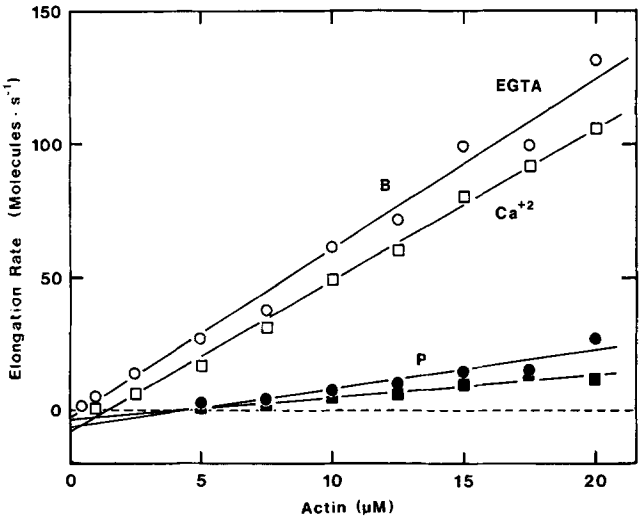

Figure 4. Elongation rates at the barbed (*open symbols*) and pointed (*closed symbols*) ends of actin filaments as a function of the actin monomer concentration. Conditions: 1 mM $MgCl_2$, 50 μM $CaCl_2$, 0.3 mM ATP, 0.25 mM DTT, 10 mM imidazole (pH 7) with either 1 mM EGTA (*circles*) or no EGTA (*squares*), 22°C.

Results

The improved methods for measuring rapid actin filament elongation rates and for preparing ADP-actin made it possible to re-investigate the elongation process at high rates and to measure the elongation rate constants for ADP-actin at both ends of the filament. Growth is linear with time (Fig. 2). Subunit addition rates up from 0.05 to at least 280 s^{-1} can now be measured routinely by electron microscopy.

In three different buffers, plots of elongation rate vs. ATP-actin monomer concentration were linear up to 20 μM actin (Figs. 3 and 4) at both ends. Under optimal conditions (50 mM KCl, 1 mM $MgCl_2$, 1 mM EGTA) with 20 μM actin the absolute rate was 280 molecules/s^{-1}. At the barbed end, the fits to straight lines were excellent with correlation

Table I. Elongation Rate Constants Measured in This Study

Conditions	Experiment	Barbed			Pointed		
		k_+	k_-	$\bar{A}_1$	k_+	k_-	$\bar{A}_1$
50 mM KCl, 1 mM $MgCl_2$ 1 mM EGTA, 0.2 mM ATP							
	A	11.3	3.0	0.26	1.0	0.5	0.50
	B	13.3	1.7	0.13	1.1	0.7	0.62
	C-1	12.6	1.2	0.10	1.2	0.7	0.57
	C-2	12.6	1.2	0.10	1.2	0.4	0.34
	C (reversed)	10.9	1.1	0.10	–	–	–
	D	10.2	0.3	0.03	1.5	1.2	0.77
	D (reversed)	10.4	1.1	0.11	1.5	1.2	0.77
	Mean	11.6	1.4	0.12	1.3	0.8	0.60
	SD	1.2	0.8	0.07	0.2	0.3	0.17
50 mM KCl, 1 mM $MgCl_2$ 1 mM EGTA, 0.2 mM ADP							
	C	3.7	6.2	1.7	0.15	0.22	1.5
	D	3.8	8.1	2.1	0.17	0.31	1.8
	Mean	3.8	7.2	1.9	0.16	0.27	1.7
1 mM $MgCl_2$, 1 mM EGTA, 0.3 mM ATP							
	E	5.3	2.4	0.55	1.0	5.7	5.7
	F	6.4	3.4	0.54	1.5	6.8	4.6
	Mean	5.9	2.9	0.55	1.3	6.3	5.2
1 mM $MgCl_2$, 50 μM $CaCl_2$, 0.3 mM ATP							
	G	5.7	8.6	1.5	0.8	3.7	4.5

Units: k_+ ($\mu M^{-1}s^{-1}$); k_- (s^{-1}); $\bar{A}_1$ (μM). (*reversed*) signifies samples of Mg-ATP-actin that were converted to Mg-ADP-actin and then reversed back to Mg-ATP-actin.

coefficients of 0.993 to 0.998. The data for the pointed ends fit to straight lines with correlation coefficients of 0.95 to 0.99. The larger scatter in the data for the pointed end is attributable to the difficulty in measuring the length of the short bundles at that end and to the fact that growth at that end is more irregular than at the barbed end. The standard deviation of the lengths was usually 10–20% of the mean at the barbed end, but usually 15 to 30% at the pointed end. The frequency of APs with growth at the barbed end was close to 100% at all time points, while in the worst case up to 40% of the pointed ends did not exhibit growth at the earliest time point. At later time points up to 90% of the APs grew at both ends. For unknown reasons, a small fraction of the pointed ends never grew and others started only after a delay of a few seconds.

The slopes and intercepts of these plots give the association and dissociation rate constants at the two ends (Table I). These values for the rate constants are based on much more extensive data than previous electron microscopic measurements (Pollard and Mooseker, 1981; Bonder et al., 1983; Coluccio and Tilney, 1984) but confirm the main conclusions from that work. In ATP, KCl, $MgCl_2$, and EGTA, the mean association rate constant at the barbed end is 11.6 $\mu M^{-1}s^{-1}$. The mean dissociation rate constant is 1.4 s^{-1}. At the pointed end the rate constants are 1.3 $\mu M^{-1}s^{-1}$ and 0.8 s^{-1}. These values were highly reproducible over five separate experiments. The mean critical concentrations are 0.12 μM at the barbed end and 0.60 μM at the pointed end. Under these conditions the critical concentration in bulk samples is 0.14 μM (Drenckhahn and Pollard, 1986).

In $MgCl_2$ and ATP without KCl, the association rate con-

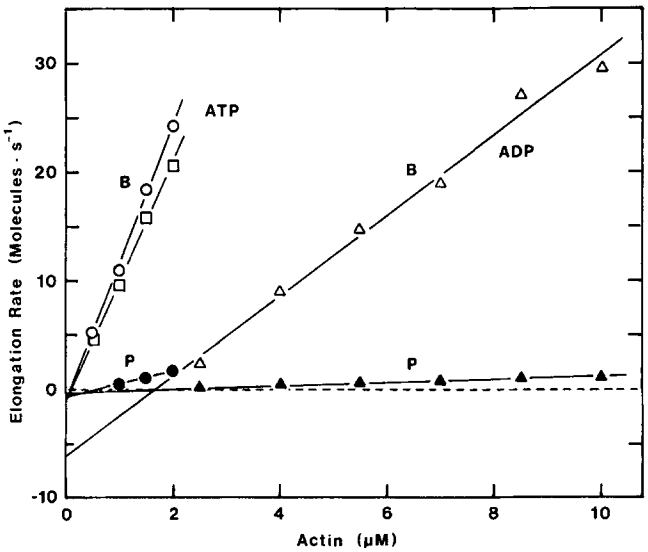

Figure 5. Elongation rates at the barbed (*open symbols*) and pointed (*solid symbols*) ends of actin filaments as a function of the concentration of ATP-actin (*open and solid circles, open squares*) and ADP-actin (*open and solid triangles*). Conditions: 50 mM KCl, 1 mM $MgCl_2$, 1.1 mM EGTA, 0.5 mM DTT, 22°C. As described in detail in Materials and Methods, Mg-ATP-actin (*circles*) was treated with hexokinase and glucose to convert it to Mg-ADP-actin (*triangles*) and then at the completion of the experiments with Mg-ADP-actin, it was reconverted to Mg-ATP-actin (*open squares*) with excess ATP. The pointed end rates with Mg-ATP-actin before and after conversion to Mg-ADP-actin were the same.

stant at the barbed end is ~6 $\mu M^{-1}s^{-1}$ ± Ca^{++}, while the dissociation rate constant is greater in Ca^{++} than in EGTA (Table I, Fig. 4). At the pointed end the association rate constants in $MgCl_2$ ± Ca^{++} are similar to those in KCl-$MgCl_2$-EGTA, but these dissociation rate constants are more than five times larger without KCl (Table I). Consequently the critical concentrations at the pointed end in $MgCl_2$ alone (~5 μM) are much larger than in KCl-$MgCl_2$.

The improved method for exchanging ATP and ADP bound to actin monomers (Selden et al., 1986) made it possible to compare directly, with the same preparation of actin, the elongation reactions of ADP-actin and ATP-actin. Under the conditions used, full activity of the actin was preserved during the exchange of ATP for ADP, since re-exchange of ADP for ATP produced actin monomers with the same elongation properties as the starting material (Fig. 5).

As expected from theoretical considerations, the critical concentrations for ADP-actin at the two ends are the same (within 10%) (Fig. 5; Table I). For these ADP-actin preparations, the critical concentration at the barbed end is ~20 times higher than for ATP-actin in KCl-$MgCl_2$-EGTA (Fig. 4). At the barbed end, the association rate constant of ADP-actin is one third that for ATP-actin while the dissociation constant is about five times larger (Table I). This was expected from previous measurements with bulk samples where reactions at the barbed end predominate (Pollard, 1984; Carlier et al., 1984; Lal et al., 1984*a*, *b*). At the pointed end, both the association and dissociation rate constants for ADP-actin are less than for ATP-actin (Table I), as predicted from studies with bulk samples (Pollard, 1984).

Discussion

Comparison of Values for the Elongation Rate Constants

For ATP-actin, there is general agreement among the electron microscopic measurements of the elongation rate constants using bundles of actin filaments as nuclei (Table II). Nuclei consisting of individual actin filaments decorated with myosin heads give similar results (see Table III in Pollard and Cooper, 1986). Spectroscopic methods with bulk samples have, in general, given lower absolute values for the rate constants but approximately the same ratios of k_-/k_+. It is difficult to conceive how the EM measurements could give erroneously high growth rates, so the lower values from bulk samples are probably attributable to over estimates of the number of growing polymers in these experiments. The limited data available on ADP-actin is also consistent with EM giving proportionally higher values, at least in KCl-$MgCl_2$-EGTA.

The good correspondence of the values obtained by such different methods supports the validity of both the electron microscopic and spectroscopic methods. The electron microscopic method is much more tedious than the spectroscopic method, but it has two important advantages. Electron microscopy gives the absolute rate of growth directly and allows one to measure growth at both ends simultaneously without the use of molecules that cap one of the ends. In my hands (Pollard, 1983), the spectroscopic method is ~100 times faster than electron microscopy and potentially more

Table II. Comparison of Elongation Rate Constants from Different Studies

		ATP						ADP						
		Barbed			Pointed			Barbed			Pointed			
Conditions	Method	k_+	k_-	$\bar{A}_1$	k_+	k_-	$\bar{A}_1$	k_+	k_-	$\bar{A}_1$	k_+	k_-	$\bar{A}_1$	Reference
	(nucleus)													
50–100 mM KCl	*EM*													
1–5 mM Mg^{++}	(microvillar cores)	8.8	2.0	0.23	2.2	1.4	0.64	–	–	–	–	–	–	A
	(acrosomal processes)	12.3	2.0	0.16	1.5	0.7	0.5	–	–	–	–	–	–	B
	(acrosomal processes)	3.4	0.3	0.10	0.3	0.3	1.0	–	–	–	–	–	–	C
	(acrosomal processes)	11.6	1.4	0.12	1.3	0.8	0.60	3.8	7.2	1.9	0.16	0.27	1.7	D
	Fluorescence													
	(trimers)	5.2	0.4	0.07	–	–	–	0.9	1.8	2.0	–	–	–	E
1 mM $MgCl_2$	*EM*													
0.1 mM $CaCl_2$	(acrosomal processes)	5.7	8.6	1.5	0.8	3.7	4.5	–	–	–	–	–	–	D
	Fluorescence													
	(trimers)	1.7	0.2	0.14	–	–	–	0.8	6.0	8.0	–	–	–	E, F
	(actin-gelsolin)	–	–	–	0.02	0.05	2.9	–	–	–	–	–	–	G
	(actin-gelsolin)	–	–	–	0.1	0.4	4.0	–	–	–	0.05	0.4	8.0	F
	(filaments ± cytochalasin D)	1.4	0.14*–4.6	0.1*–3.3	0.12	0.45	3.8	0.75	6.0	8.0	0.05	0.43	8.0	H
1 mM $MgCl_2$	*EM*													
1 mM EGTA	(acrosomal processes)	5.9	2.9	0.50	1.3	6.3	4.9	–	–	–	–	–	–	D

Units: k_+ ($\mu M^{-1}s^{-1}$); k_- (s^{-1}); $\bar{A}_1$ (μM).
* A range of values were given, with the lowest values measured at low actin monomer concentrations.
References: (*A*) Pollard and Mooseker, 1981; (*B*) Bonder et al., 1983; (*C*) Coluccio and Tilney, 1984; (*D*) present report; (*E*) Lal et al., 1984*a*, *b*; (*F*) Coue and Korn, 1985; (*G*) Doi and Frieden, 1984; (*H*) Carlier et al., 1986*a*.

accurate because the signal is both continuous and the average of many more filaments. Furthermore, spectroscopy can be used to measure both positive and negative rates, while electron microscopy has thus far only been successful with positive rates. On the other hand, attempts to measure events at the pointed end spectroscopically with capped filaments have been difficult as elaborated in the next paragraph.

For the following discussion of the mechanism of elongation, a key point hinges on the relative rates of dissociation of ATP-actin and ADP-actin from the two ends of the filament. There is agreement that ADP-actin dissociates at least five times faster from the barbed end than ATP-actin (Table II). My EM measurements show that the opposite is true at the pointed end, at least in KCl-$MgCl_2$-EGTA, where ATP-actin dissociates about three times faster than ADP-actin. On the other hand, spectroscopic experiments in $MgCl_2$ with gelsolin (Coue and Korn, 1985) or cytochalasin D (Carlier et al., 1986*a*) to block the barbed ends of filaments (Table II), suggested that the dissociation constants for ATP-actin and ADP-actin at the pointed end are about the same. However, with both cytochalasin and gelsolin the dependence of the elongation rate on the concentration of actin was nonlinear above the critical concentration, making it impossible to be certain about the value of the dissociation constant for ATP-actin. An alternate interpretation consistent with my electron microscopy results is that the slope of these plots changes near the critical concentration because ATP-actin is the predominant terminal species in that range and because the association and dissociation rate constants are larger for ATP-actin than ADP-actin. This point deserves further investigation to learn whether the disagreement is attributable to the difference in conditions or whether either the spectroscopic or electron microscopic measurements are in error.

The Mechanism of Elongation

The earliest measurements of the elongation rate constants by electron microscopy of individual filaments (Pollard and Mooseker, 1981; Bonder et al., 1983) and by spectroscopic methods on bulk samples (Pollard, 1983; Lal et al., 1984*a*) were restricted to relatively low positive reaction rates and all reported linear plots of elongation rate vs. concentration of ATP-actin above the critical concentration. This data was consistent with the simple model for elongation proposed by Oosawa and Asakura (1975). The elongation rate at the end of a filament was simply

$$R = k_+(A_1) - k_-, \quad (1)$$

where k_+ is the association rate constant, k_- is the dissociation rate constant, and A_1 is the actin monomer concentration. The values of the rate constants were quite different at the two ends, but even in a bulk sample with many filaments growing at both ends the elongation rate was expected to have a linear dependence on the concentration of actin monomers, since it was the sum of two apparently linear reactions.

This simple model had to be modified when it was found that ADP-actin dissociates faster from the barbed end than ATP-actin (Pollard, 1984; Carlier et al., 1984; Lal et al., 1984*b*) with the consequence that, even in ATP, plots of elongation rate vs. actin concentration curve down toward the ADP-actin dissociation rate below the critical concentration (Carlier et al., 1984). There is now general agreement that the nonlinearity in the negative arm of these plots is due to the increase toward 100% in the fraction of ADP subunits dissociating from the barbed end as the ATP-actin monomer concentration approaches zero.

Subsequently, Carlier et al. (1985) found for bulk samples that at actin concentrations well above the critical concentration, the plots of elongation rate vs. ATP-actin concentration curve upward. They interpreted this nonlinearity in the positive part of the plot as a sharp but small change in the slope at 11 μM actin in 1 mM $MgCl_2 \pm Ca^{++}$. Both above and below 11 μM, the plots of rate vs. concentration appeared linear, but the upper arm of the plot had a larger slope (see Fig. 6 in Carlier et al., 1984, and Fig. 2 in Pantaloni et al., 1985*b*). At actin concentrations above 11 μM, the association rate constant was 10–20% larger and the dissociation rate constant was five times larger than at lower actin concentrations. Recently Carlier et al. (1986*b*) reported the results of a similar experiment in the KCl-$MgCl_2$-EGTA buffer used in this paper. Again a three-phase plot was obtained, but the break in the positive arm of the plot was at 0.9 μM actin rather than 11 μM. It is important to note that these results were obtained with bulk samples where both ends contributed to the elongation process.

There are now two explanations for the complex three-phase dependence of the elongation rate on ATP-actin concentration. The first proposed by Pantaloni et al. (1985*a*, *b*) argues that the nucleotide composition of subunits near the end of the filament varies with elongation rate and this influences both the association and dissociation rate constants. I suggest that the break in the positive part of the plots is simply due to the added contribution of elongation at the pointed end above its critical concentration. For this to be true, the pointed end must be relatively inert below its critical concentration as observed here.

The Pantaloni model postulates that ATP bound to polymerized actin subunits is hydrolyzed at a relatively high rate at the interface between the ADP-actin core of the filament and the actin-ATP caps at the two ends, but not on the two terminal subunits. At actin concentrations just above the critical concentration, hydrolysis is fast enough to keep up with elongation so that the ATP cap consists of only two or a few subunits. Above 11 μM ATP-actin, they suggested that the elongation rate exceeds the hydrolysis rate so that subunit association would be exclusively between ATP-actin monomers and polymer ends with long ATP caps. According to this model, the association and dissociation rate constants depend on the length of the ATP cap, so naturally the slope of the plots changes above 11 μM actin. The model includes the concept that ATP-actin binds 10 times weaker to ends with long ATP caps than short ATP caps, a conclusion based on the critical concentration measured spectroscopically in solutions of continuously sonicated ATP-actin (Carlier et al., 1985). Theoretical plots using some experimental values for constants fit the complex, three-phase elongation rate plots remarkably well.

I propose a simple model that differs from the Pantaloni model in two major aspects: (*a*) the rates of subunit association and dissociation depend almost exclusively on the nucleotide composition of the adding or departing actin molecule; and (*b*) the elongation in bulk samples is the sum of substantially different reactions at the two ends. (The nucleotide composition of the subunits at or near the end of the fila-

ment may affect the reaction rates, but this is not detectable with current methods.) As elaborated below, this model can also account for the complex, three-phase dependence of the bulk elongation rate on actin concentration (Carlier et al., 1985, 1986*b*).

My model is based on the following assumptions. (*a*) Association and dissociation of subunits at each end is by the Oosawa mechanism (Eq. 1). (*b*) The rate of ATP hydrolysis is relatively low on the terminal subunit. This is justified in a later paragraph for the kinetically more important barbed end. Consequently, above the critical concentration ATP-actin will be the predominant dissociating species. (*c*) Below the critical concentration the fraction of terminal subunits with bound ATP is proportional to the rate of association of ATP-actin. Therefore, the fraction with ATP is directly proportional to the concentration of ATP-actin monomers. In other words, the fraction of ATP ends is 0 when the monomer concentration is 0 and 1.0 at and above the critical monomer concentration. This is, of course, an over-simplification, but scaling this parameter differently will give qualitatively similar results for the combined behavior of the two ends. Thus the rate of change of length at the two ends in ATP-actin is

$$R^B = k_+^{BT}A_1^T + k_+^{BD}A_1^D - f^{BT}k_-^{BT} - f^{BD}k_-, \quad (2)$$

$$R^P = k_+^{PT}A_1^T + k_+^{PD}A_-^D - f^{PT}k_-^{PT} - f^{PD}k_-^{BD}. \quad (3)$$

The superscripts are as follows: B for barbed end, P for pointed end, T for ATP, and D for ADP. The fractional nucleotide composition of the terminal subunits are represented by f. Since $A_1^D = 0$, the second term in each equation drops out. The net elongation rate in bulk samples is simply

$$\frac{dA_p}{dt} = N(R^B + R^P), \quad (4)$$

where A_p is the concentration of polymerized actin and N is the concentration of filaments.

Using these equations, the assumptions stated above and the rate constants from Table I, I have calculated the elongation rates at each end as a function of the monomer concentration (Fig. 6). Note that the depolymerization rate at the barbed end increases nonlinearly as the monomer concentration approaches zero due to the rapid dissociation of ADP-actin that constitutes a large fraction of the ends as A_1^T goes to zero. Note also that the dependence of the depolymerization rate on the actin concentration at the pointed end is quite different. There is a minimum in the curve between $A_1 = 0$ and the critical concentration, since ADP-actin dissociates slower than ATP-actin from the pointed end.

When the elongation rates at the two ends are summed to obtain the net rate, one obtains a complex, three-phase plot (Fig. 6) like that observed by Carlier et al. (1985, 1986*b*) for bulk samples. The important features are a critical concentration very close to that for the barbed end, a nonlinear negative arm below the critical concentration that reaches the dissociation rate for ADP-actin at the barbed end, and a nonlinear positive arm above the critical concentration that bends upward at ~0.6 μM, the critical concentration for the pointed end. The key elements producing this behavior are the large off rate for ADP-actin at the barbed end, the large difference in the critical concentrations at the two ends, and

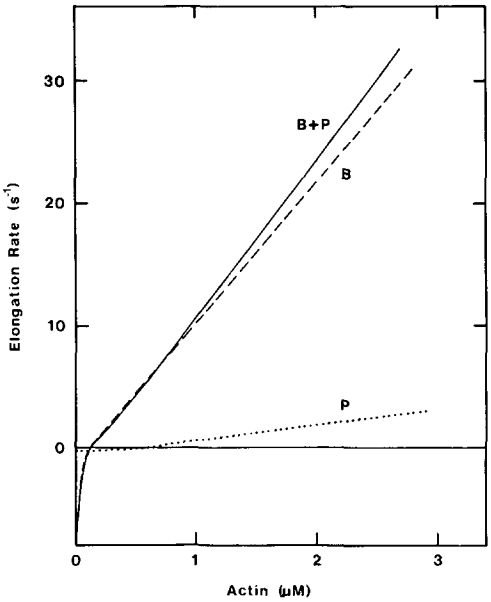

Figure 6. Theoretical plots of elongation rates as a function of ATP-actin monomer concentration. Barbed end (*dashed line*); point end (*dotted line*); sum of two ends (*solid line*). The assumptions are that (*a*) all association reactions are by ATP-actin monomers; (*b*) above the critical concentrations, the dissociation reactions are ATP-actin subunits; (*c*) below the critical concentration for each end the fraction of dissociating subunits with bound ATP is directly proportional to free monomer concentration/critical concentration and both ATP-actin and ADP-actin dissociate from the end at their characteristic rates. KCl-Mg-EGTA buffer as in Fig. 3. k_+^{BT} = 11.6; k_-^{BT} = 1.4; k_+^{PT} = 1.3; k_-^{PT} = 0.8; k_-^{PD} = 0.27 as measured.

the relative inertness of the pointed end below its critical concentration. The sum of the rates at the two ends is almost identical if slightly different assumptions are made about the nucleotide composition at the pointed end. For example, if hydrolysis is tightly coupled to binding as proposed by Coue and Korn (1985), then below the critical concentration all of the dissociating subunits will have ADP and that part of the plot will be linear as observed (Coue and Korn, 1985; Carlier et al., 1986*a*). At or just above the critical concentration the slope will change as a higher fraction of ends are occupied by at least one ATP-actin.

Similar calculations for actin in 1 mM $MgCl_2$, using the rate constants measured by electron microscopy for ATP-actin and rate constants for ADP-actin proportional to those measured in KCl-$MgCl_2$-EGTA, produce a dependence of polymerization rate on ATP-actin concentration remarkably similar to the observations of Carlier et al. (1985), except that the inflection in the positive arm is at 4 μM rather than 11 μM. Carlier et al. (1985) selected 11 μM actin for the inflection point of the positive arm of their plots largely to include 3 μM as the value of the critical concentration for the "ATP-equilibrium polymer." I have used least squares linear regression to fit their experimental data to a straight line and find that the fit is actually better with the inflection point between 3 and 5 μM rather than at 11 μM, so my theoretical plots are consistent with their data. My model is also consistent with the absence of an inflection in the positive arm of such plots for Ca^{++}-actin (Carlier et al., 1986*b*), since the critical concentrations at the two ends are the same (Pollard and Mooseker, 1981).

How well do the two models account for the available experimental data? Both can explain the complex dependence of the elongation rate of bulk samples on the concentration of ATP-actin. My model is consistent with the linear dependence of the elongation rate at both ends on ATP-actin concentration above the critical concentration (Figs. 3–5). The Pantaloni model is not consistent with this data. Providing that my data are correct and given that the derivation of the Pantaloni model is formally correct, this inconsistency is probably attributable to error in one or more of the assumptions required to formulate the model. The absence of a break in the positive arm of these plots (Figs. 3–5) also suggests that the concept of an "ATP-equilibrium polymer" under continuous sonication (Carlier et al., 1985) needs to be re-examined. The rate constants for binding and dissociation of ATP-actin to filaments at high elongation rates (where there must be a large ATP cap) give a critical concentration far below that observed during sonication. The exchange of subunits under sonication may include reactions (such as annealing and dissociations of ADP-actin from broken ends) that were not anticipated in the earlier study. The Pantaloni model is superior to mine in one way; it can account for the kinetic overshoot in the extent of polymerization in the presence of capping proteins (e.g., Coue and Korn, 1985). My model does not speak to this interesting point.

Events at Steady State

The availability of the minimal set of eight rate constants for subunit association and dissociation at the two ends makes it possible to predict some of the events at steady state in ATP. First, assuming that the concentration of ADP-actin is zero and using the rate constants in Table I one can calculate what fraction of terminal subunits would have to hydrolyze their ATP before dissociation to yield any steady-state critical concentration. The result is that the hydrolysis rate constant must be $<0.2\ s^{-1}$ to account for the critical concentration of 0.14 μM observed in bulk samples in KCl-$MgCl_2$-EGTA (Drenckhahn and Pollard, 1986).

Second, the rate constants (Table I) can be used to put some limits on the subunit exchange rates. Since the critical concentrations differ at the two ends, there will be a flux of subunits from the barbed end to the pointed end, although the exact rate will depend on the rate of hydrolysis of ATP on the terminal subunits at each end of the filament, rates that are not yet established. Further, as discussed previously (Pollard, 1984), there will be minor fluctuations in the length of the barbed end when all of the terminal subunits occasionally have bound ADP and these subunits transiently dissociate rapidly until the next ATP subunit binds to and stabilizes the end. The new rate constants show that the pointed end will be relatively stable, since the dissociation constants are low for both ATP- and ADP-actin, as first indicated by Coluccio and Tilney (1983).

I thank Drs. Lynn Selden and Jim Estes for providing me with the details of their new method to prepare ADP-actin; Dr. M.-F. Carlier and John Cooper for discussions of the elongation mechanism; and the referees for raising a number of thought provoking questions about the mechanism of elongation.

This work was supported by Research Grant GM-26338 from the National Institutes of Health and a Research Grant from the Muscular Dystrophy Association of America.

Received for publication 26 July 1986, and in revised form 22 September 1986.

Note Added in Proof. Readers of this paper will be interested in a new paper (from Keiser, T., A. Schiller, and A. Wegner, 1986, *Biochemistry*, 25:4899–4906) titled "Nonlinear increase of elongation rate of actin filaments with actin monomer concentration." These authors consider some new models to explain the complex properties of the actin filament elongation reaction.

References

Bonder, E. M., D. J. Fishkind, and M. S. Mooseker. 1983. Direct measurement of critical concentrations and assembly rate constants at the 2 ends of an actin filament. *Cell.* 34:491–501.

Carlier, M.-F., P. Criquet, D. Pantaloni, and E. D. Korn. 1986*a*. Interaction of cytochalasin-D with actin filaments in the presence of ADP and ATP. *J. Biol. Chem.* 261:2041–2050.

Carlier, M.-F., D. Pantaloni, and E. D. Korn. 1984. Evidence for an ATP cap at the ends of actin filaments and its regulation of the F-actin steady state. *J. Biol. Chem.* 259:9983–9986.

Carlier, M.-F., D. Pantaloni, and E. D. Korn. 1985. Polymerization of ADP-actin and ATP-actin under sonication and characterization of the ATP-actin equilibrium polymer. *J. Biol. Chem.* 260:6565–6571.

Carlier, M.-F., D. Pantaloni, and E. D. Korn. 1986*b*. The effects of Mg^{2+} at the high-affinity and low-affinity sites on the polymerization of actin and associated ATP hydrolysis. *J. Biol. Chem.* 261:10785–10792.

Coluccio, L. M., and L. G. Tilney. 1983. Under physiological conditions actin disassembles slowly from the nonpreferred end of an actin filament. *J. Cell Biol.* 97:1629–1634.

Coluccio, L. M., and L. G. Tilney. 1984. Phalloidin enhances actin assembly by preventing monomer dissociation. *J. Cell Biol.* 99:529–535.

Coue, M., and E. D. Korn. 1985. Interaction of plasma gelsolin with G-actin and F-actin in the presence and absence of calcium-ions. *J. Biol. Chem.* 260: 15033–15041.

Doi, Y., and C. Frieden. 1984. Actin polymerization—the effect of brevin on filament size and rate of polymerization. *J. Biol. Chem.* 259:1868–1875.

Drenckhahn, D., and T. D. Pollard. 1986. Elongation of actin filaments is a diffusion-limited reaction at the barbed end and is accelerated by inert macromolecules. *J. Biol. Chem.* 261:12754–12758.

Frieden, C. 1985. Actin and tubulin polymerization—the use of kinetic methods to determine mechanism. *Annu. Rev. Biophys.* 14:189–210.

Korn, E. D. 1982. Actin polymerization and its regulation by proteins from non-muscle cells. *Physiol. Rev.* 62:672–737.

Lal, A. A., S. L. Brenner, and E. D. Korn. 1984*a*. Preparation and polymerization of skeletal muscle ADP-actin. *J. Biol. Chem.* 259:13061–13065.

Lal, A. A., E. D. Korn, and S. L. Brenner. 1984*b*. Rate constants for actin polymerization in ATP determined using cross-linked actin trimers as nuclei. *J. Biol. Chem.* 259:8794–8800.

MacLean-Fletcher, S., and T. D. Pollard. 1980. Identification of a factor in conventional muscle actin preparations which inhibits actin filament self-association. *Biochem. Biophys. Res. Commun.* 96:18–27.

Oosawa, F., and S. Asakura. 1975. Thermodynamics of the Polymerization of Protein. Academic Press, Inc. New York. 204 pp.

Pantaloni, D., M. F. Carlier, and E. D. Korn. 1985*a*. The interaction between ATP-actin and ADP-actin—a tentative model for actin polymerization. *J. Biol. Chem.* 260:6572–6578.

Pantaloni, D., T. L. Hill, M. F. Carlier, and E. D. Korn. 1985*b*. A model for actin polymerization and the kinetic effects of ATP hydrolysis. *Proc. Natl. Acad. Sci. USA.* 82:7207–7211.

Pollard, T. D. 1983. Measurement of rate constants for actin filament elongation in solution. *Anal Biochem.* 134:406–412.

Pollard, T. D. 1984. Polymerization of ADP-actin. *J. Cell Biol.* 99:769–777.

Pollard, T. D., and J. A. Cooper. 1984. Quantitative analysis of the effect of Acanthamoeba profilin on actin filament nucleation and elongation. *Biochemistry.* 23:6631–6641.

Pollard, T. D., and J. A. Cooper. 1986. Actin and actin-binding proteins. A critical evaluation of mechanisms and functions. *Annu. Rev. Biochem.* 55: 987–1035.

Pollard, T. D., and M. S. Mooseker. 1981. Direct measurement of actin polymerization rate constants by electron microscopy of actin filaments nucleated by isolated microvillus cores. *J. Cell Biol.* 88:654–659.

Pollard, T. D., and A. G. Weeds. 1984. The rate constant for ATP hydrolysis by polymerized actin. *FEBS (Fed. Eur. Biochem. Soc.) Lett.* 170:94–98.

Selden, L. A., L. C. Gershman, and J. E. Estes. 1986. Cation considerations in the preparation and characterization of monomeric ADP-actin. *Biophys. J.* 49(2, Pt. 2):454a.

Selve, N., and A. Wegner. 1986. Rate of treadmilling of actin filaments in vitro. *J. Mol. Biol.* 187:627–631.

Spudich, J. A., and S. Watt. 1971. The regulation of rabbit skeletal muscle contraction. I. Biochemical studies of the interaction of the tropomyosin-troponin complex with actin and the proteolytic fragments of myosin. *J. Biol. Chem.* 246:4866–4871.

Tilney, L. G. 1975. Actin filaments in the acrosomal reaction of *Limulus* sperm. Motion generated by alterations in the packing of the filaments. *J. Cell Biol.* 64:289–310.